J|A|C|S
ARTICLES
Published on Web 01/19/2002

First Systematic Band-Filling Control in Organic Conductors

Hatsumi Mori,*,† Masakazu Kamiya,†,‡ Masamitsu Haemori,†,‡ Hideaki Suzuki,†,§ Shoji Tanaka,† Yutaka Nishio,‡ Kohji Kajita,‡ and Hiroshi Moriyama§

Contribution from the International Superconductivity Technology Center (ISTEC), Shinonome Koto-ku, Tokyo 135-0062, Japan, Department of Physics, Faculty of Science, Toho University, Miyama, Chiba 274-8510, Japan, and Department of Chemistry, Faculty of Science, Toho University, Miyama, Chiba 274-8510, Japan

Received March 2, 2001

Abstract: The systematic study of band-filling control for *four* kinds of organic conductors with various kinds of ground states has succeeded. (1) By partial substitution of $(GaCl_4)^-$ by $(MCl_4)^{2-}$ [M = Co, Zn] in the anion blocking layer of λ-$ET_2(GaCl_4)^-$ [ET = bis(ethylenedithio)tetrathiafulvalene], single crystals of λ-$ET_2(GaCl_4)^-_{1-x}(MCl_4)^{2-}_x$ [x = 0.0, 0.05, 0.06] have been obtained. The resistivity at room temperature decreases from 3 Ω cm (x = 0.0) to 0.1 Ω cm (x = 0.06) by doping to the antiferromagnet with an effective half-filled band (x = 0.0). (2) Another 2:1 (donor/anion) salt, δ'-$ET_2(GaCl_4)^-$, which is a spin gap material, has been doped as δ'-$ET_2(GaCl_4)^-_{1-x}(MCl_4)^{2-}_x$ [x = 0.05, 0.14]. The resistivity is lowered from 10 Ω cm (x = 0.0) to 0.3 Ω cm (x = 0.14). For both 2:1 salts, the semiconducting behaviors have transferred to relatively conductive semiconducting ones by doping. (3) As for α-type 3:1 salts, the parent material is in a charge-ordering state such as α-$(ET^+ET^+ET^0)(CoCl_4)^{2-}$(TCE), where the charge-ordered donors are dispersed in the two-dimensional conducting layer. Although the calculation of α-$ET_3(CoCl_4)^{2-}$(TCE) shows a band-insulating nature, and the crystal structure analysis indicates that this material is in a charge-ordering state, the metallic behavior down to 165 K has been observed. With doping of $(GaCl_4)^-$ to the α-system, isostructural α-$ET_3(CoCl_4)^{2-}_{1-x}(GaCl_4)^-_x$(TCE) [$x$ = 0.54, 0.57, 0.62] have been afforded, where the pattern of the horizontal stripe-type charge ordering changes with an increase of x. (4) By doping $(GaCl_4)^-$ to the 3:2 gapless band insulator which is isostructural to β'-$ET_3(MCl_4)_2^{2-}$ [M = Zn, Mn], the obtained β'-$ET_3(CoCl_4)^{2-}_{2-x}(GaCl_4)^-_x$ [x = 0.66, 0.88] shows metallic behavior down to 100 and 140 K, respectively. They are the first metallic states in organic conductors by band-filling control of the gapless band insulator. These systematic studies of band-filling control suggest that the doping to the gapless band insulator with a *pseudo*-1/2-filled band is most effective.

Introduction

The electronic states of conductors, including superconductors, are usually controlled by (1) *electron correlation control* (U/W, U = on-site Coulomb repulsion, W = bandwidth) or/and (2) *band-filling control*. In an *organic* system, the superconducting state has *not* been obtained by band-filling control, but by electron correlation control; the ground state of $TMTCF_2X$ (C = S, Se), pseudo-one-dimensional conductors, has been changed from nonmagnetic, commensurate SDW, incommensurate SDW, superconducting, to a metallic state by applying chemical and physical pressure, namely, electron correlation control.[1] Strictly speaking, the dimensionality of this system slightly increases with application of pressure in the regime of pseudo-one-dimensionality, and the electron−phonon coupling is also an important parameter in the $TMTCF_2X$ system.

As for κ-ET_2X, two-dimensional conductors, the superconducting state has been obtained by the suppression of the antiferromagnetic state with *chemical and physical electron correlation control*.[2] For θ-ET_2X with a two-dimensional 3/4-filled band structure, the proposed phase diagram indicates that the superconducting state has been reached by the suppression of charge and spin fluctuations with chemical electron correlation control.[3] As for λ-D_2GaCl_4, [D = ET, BEDT-STF (bis(ethylenedithio)selenathiafulvalene),[4] and BETS (bis(ethylenedithio)tetraselenafulvalene)[5]], our group has proposed that the superconducting state of λ-$BETS_2GaCl_4$ has been obtained by chemical electron correlation control of λ-D_2GaCl_4, [D = ET, BEDT-STF], substituting the S atoms by the Se atoms with a larger orbital in the fulvalene frames.[6]

* To whom correspondence should be addressed. Phone: +81-3-3536-0618 (ext 221). Fax: +81-3-3536-5714. E-mail: mori@istec.or.jp.
† ISTEC.
‡ Department of Physics, Toho University.
§ Department of Chemistry, Toho University.

(1) Jerome, D. *Science* **1991**, *252*, 1509; Moser, J.; Gabay, M.; Auban-Senzier, P.; Jerome, D.; Bechgaard, K.; Fabre, J. M. *Eur. Phys. J.* **1998**, *B1*, 39.
(2) Kanoda, K. *Hyperfine Interact.* **1997**, *104*, 235.
(3) Mori, H.; Tanaka, S.; Mori, T.; Maruyama, Y. *Bull. Chem. Soc. Jpn.* **1995**, *68*, 1136; Mori, H.; Tanaka, S.; Mori, T. *J. Phys. I* **1996**, *6*, 1987. Mori, T.; Fuse, A.; Mori, H.; Tanaka, S. *Physica C* **1996**, *264*, 22. Mori, H.; Tanaka, S.; Mori, T.; Kobayashi, A.; Kobayashi, H. *Bull. Chem. Soc. Jpn.* **1998**, *71*, 797. Mori, H.; Tanaka, S.; Mori, T. *Phys. Rev. B* **1998**, *57*, 12023.
(4) Naito T.; Kobayashi H.; Kobayashi, A. *Bull. Chem. Soc. Jpn.* **1997**, *70*, 107.
(5) Kobayashi, A.; Udagawa, T.; Tomita, H.; Naito, T.; Kobayashi, H. *Chem. Lett.* **1993**, 2179. Tanaka, H.; Kobayashi, A.; Sato, A.; Akutsu, H.; Kobayashi, H. *J. Am. Chem. Soc.* **1999**, *121*, 760.

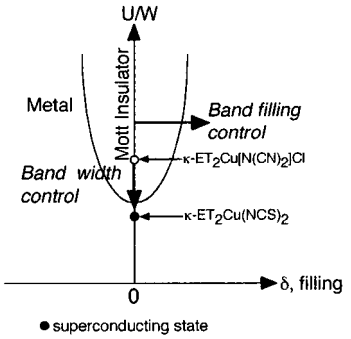

Figure 1. Electronic phase diagram of organic conductors. The arrow in the vertical direction indicates the electron correlation control (U/W, U = on-site Coulomb repulsion energy, W = bandwidth). The organic antiferromagnetic Mott insulating state [κ-$ET_2Cu[N(CN)_2]Cl$] transforms to a superconducting one [κ-$ET_2Cu(NCS)_2$] by controlling U/W. The arrow in the horizontal direction shows the band-filling control.

On the other hand, the *inorganic* superconductors have been obtained by both electron correlation and band-filling controls (carrier doping control). As for a heavy Fermion system, the superconductivity of $CePd_2Si_2$[7] has been afforded by applying physical pressure, that is, electron correlation control. It is characteristic that the superconducting transition is followed by the antiferromagnetic transition. The first superconductivity among vanadium materials is β'-$Cu_xV_2O_5$ ($x \approx 0.65$),[8] which is obtained by both band-filling control of x and applying external pressure, namely, electron correlation control. There are many examples of inorganic superconductors by *carrier doping control*: $Ba_{1-x}K_xBiO_3$,[9] $BaBi_{1-x}Pb_xO_3$,[10] high T_c CuO_2 superconductors,[11] graphite intercalation (C_8K),[12] and Na_xWO_3.[13] Especially, in high T_c superconductors, by doping to the parent antiferromagnet, $La^{3+}{}_2CuO_4$, with a substitution of La^{3+} by Sr^{2+}, the antiferromagnetic behavior has diminished and the superconducting state has appeared as an increase of x in $La^{3+}{}_{2-x}Sr^{2+}{}_x$-$CuO_4$[11] ($0.06 \le x \le 0.25$). Moreover, the typical carrier doping molecular superconductor is A_xC_{60} (A = alkali metal).[14]

However, there are a few examples whose electronic states are controlled by systematic carrier doping control in organic conductors. A substitution of a counteranion with a different charge usually resulted in a change of the crystal structure. This situation had prohibited us from a systematic investigation of electronic states by band filling. One exceptional example is $(DMeDCNQI)_2Cu_{1-x}Li_x$[15] with a partial substitution of differently charged *atoms*; by an increase of x, the metallic Cu material down to 1.3 K has changed to a semiconducting Li one systematically. Although the end materials are $(DMeDCNQI)_2Cu^{1.33+}$ and $(DMeDCNQI)_2Li^+$,[16] whether the carrier of $(DMeDCNQI)_2Cu_{1-x}Li_x$ is doped systematically or not is under investigation. Other examples are $(NMP)_{1-x}$-$(phenazine)_xTCNQ$[17] [NMP = *N*-methylphenazine], $(ET)_y$-$[(MnCl_4)_{1-x}(FeCl_4)_x]$,[17] and $[Si(Pc)O]_nX_y$.[17] The studies of $(NMP)_{1-x}(phenazine)_xTCNQ$ and $[Si(Pc)O]_nX_y$ are not carried out by using single crystals, but a crystalline powder, and the crystal structure and the stoichiometry of $(ET)_y[(MnCl_4)_{1-x}$-$(FeCl_4)_x]$ are not known yet.

To develop cation radical conductors by systematic band-filling control, λ-ET_2GaCl_4, an antiferromagnet with a two-dimensional layered structure, has been chosen as a parent material. The band-filling control has been examined by partial

Table 1. Preparation, Crystal Shape, and Doping Content (x) for λ-$ET_3(GaCl_4)_{1-x}(MCl_4)_x$, δ'-$ET_3(GaCl_4)_{1-x}(MCl_4)_x$ [M = Co, Zn], α-$ET_3(CoCl_4)_{1-x}(GaCl_4)_x$(TCE), and β'-$ET_3(CoCl_4)_{2-x}(GaCl_4)_x$

nominal ratio $(GaCl_4)^-$:$(CoCl_4)^{2-}$	total amt of electrolyte (mg)	obtained crystal	crystal shape	x
99:1	100	α-$ET_3(CoCl_4)_{0.38}(GaCl_4)_{0.62}$(TCE)	plate	0.62
99:1	300	λ-$ET_2(GaCl_4)_{0.95}(CoCl_4)_{0.05}$	needle	0.05
99:1	300	δ'-$ET_3(GaCl_4)_{0.95}(CoCl_4)_{0.05}$	stick	0.05
99:1	300	α-$ET_3(CoCl_4)_{0.43}(GaCl_4)_{0.57}$(TCE)	plate	0.57
98.75:1.25	100	δ'-$ET_3(GaCl_4)_{0.95}(CoCl_4)_{0.05}$	stick	0.05
98.75:1.25	100	α-$ET_3(CoCl_4)_{0.46}(GaCl_4)_{0.54}$(TCE)	plate	0.54
97.75:2.25	100	β'-$ET_3(CoCl_4)_{1.12}(GaCl_4)_{0.88}$	long plate	0.88
97:3	100	β'-$ET_3(CoCl_4)_{1.34}(GaCl_4)_{0.66}$	long plate	0.66
0:100	100	α-$ET_3(CoCl_4)$ (TCE)	plate	0.0

nominal ratio $(GaCl_4)^-$:$(ZnCl_4)^{2-}$	total amt of electrolyte (mg)	obtained crystal	crystal shape	x
98:2	100	λ-$ET_3(GaCl_4)_{0.94}(ZnCl_4)_{0.06}$	needle	0.06
98:2	100	δ'-$ET_3(GaCl_4)_{0.86}(ZnCl_4)_{0.14}$	stick	0.14

Table 2. Crystal Data and Experimental Details for λ-ET_2GaCl_4 and δ' -$ET_2(GaCl_4)_{1-x}(CoCl_4)_x$ [x = 0.0, 0.05]

	λ-ET_2GaCl_4	δ' -$ET_2(GaCl_4)_{0.95}(CoCl_4)_{0.05}$	δ'-$ET_2(GaCl_4)$
empirical formula	$C_{20}H_{16}GaCl_4S_{16}$	$C_{20}H_{16}Co_{0.05}Ga_{0.95}Cl_4S_{16}$	$C_{20}H_{16}GaCl_4S_{16}$
fw	980.84	980.84	980.84
shape	black needle	black needle	black
cryst syst	triclinic	triclinic	triclinic
space group	$P\bar{1}$ (no. 2)	$P\bar{1}$ (no. 2)	$P\bar{1}$ (no. 2)
a/Å	16.246(5)	15.042(4)	15.018(12)
b/Å	18.027(5)	17.837(4)	17.801(14)
c/Å	6.533(7)	6.638(3)	6.639(5)
α/deg	98.20(5)	90.62(3)	90.55(4)
β/deg	97.48(6)	91.77(3)	91.71(3)
γ/deg	112.29(2)	82.75(2)	82.81(3)
V/Å^3	1716(2)	1766(1)	1760
Z	2	2	2
R/R_w	0.080/0.083	0.062/0.046	0.063/0.049
D_c/g cm^{-3}	1.90	1.84	1.85
temp/K	298	298	
no. of reflns used	5237/10020 $\lvert I_0\rvert > 5\sigma\lvert I_0\rvert$	1448/7962 $\lvert I_0\rvert > 3\sigma\lvert I_0\rvert$	
$2\theta_{max}$/deg	60	60	
λ/Å	0.71073	0.71073	
ref	this work	this work	20

(6) Mori, H.; Kamiya, M.; Haemori, M.; Suzuki, T.; Tanaka, S.; Nishio, Y., Kajita, K., Moriyama, H. *Physica C* **2001**, *103*, 357.
(7) Raymond, S.; Jaccard, D.; Wilhelm, H.; Cerny, R. *Solid State Commun.* **1999**, *112*, 617.
(8) Ueda, Y. Personal communication.
(9) Sleight, A. W.; Gillson, J. L.; Biersted, P. E. *Solid State Commun*. **1975**, *17*, 27.
(10) Mattheiss, L. F.; Gyorgy, E. M.; Johnson, D. W., Jr. *Phys. Rev. B* **1988**, *37*, 3745. Cava, R. J.; Batlogg, B.; Krajewski, J. J.; Farrow, R.; Rupp, L. Q., Jr.; White, A. E.; Short, K.; Peck, W. F.; Kometani, T. *Nature* **1988**, *332*, 814.
(11) Takagi, H.; Tokura, Y.; Uchida, S. *Physica C* **1989**, *162*−*164*, 1001.
(12) Hanney, N. B.; Geballe, T. H.; Matthias, B. T.; Andres, K.; Schmidt, P.; MacNair, D. *Phys. Rev. Lett.* **1965**, *14*, 225.
(13) Garif'yanov, N. N.; Khlebnikow, S. Y.; Khlebnikov, I. S.; Garifullin, I. A. *J. Phys.* **1996**, *46*, 855.
(14) Hebard, A. F.; Rosseinsky, M. J.; Haddon, R. C.; Murphy, D. W.; Glarum, S. H.; Palstra, T. T. M.; Ramirez, A. P.; Kortan, A. R. *Nature* **1991**, *350*, 600. Tanigaki, K.; Ebbesen, T. W.; Saito, S.; Mizuki, J.; Tsai, J. S.; Kubo, Y.; Kuroshima, S. *Nature* **1991**, *352*, 222. Yildirim, T.; Barbedette, L.; Fischer, J. E.; Lin, C. L.; Robert, J.; Petit, P.; Palstra, T. T. M. *Phys. Rev. Lett.* **1996**, *77*, 167.
(15) Yamamoto, T.; Tajima, H.; Yamaura, J.; Aonuma S.; Kato R. *J. Phys. Soc. Jpn.* **1999**, *68*, 1384.
(16) Aumüller, A.; Erk, P.; Klebe, G.; Hunig, S.; von Schütz, J. U.; Werner, H.-P. *Angew. Chem., Int. Ed. Engl.* **1986**, *25*, 740. Kato, R.; Kobayashi, H.; Kobayashi, A.; Mori, T.; Inokuchi, H. *Chem. Lett.* **1987**, 1579. Hunig, S.; Erk, P. *Adv. Mater.* **1991**, *3*, 225. Hünig, S.; Kemmer, M.; Meixner, H.; Sinzger, K.; Wenner, H.; Bauer, T.; Tillmanns, E.; Lux, F. R.; Hollstein, M.; Gross, H−G.; Langohr, U.; Werner, H.-P.; von Schütz, J. U.; Wolf, H. C. *Eur. J. Inorg. Chem.* **1999**, 899.
(17) Epstein, A. J.; Miller, J. S. *Solid State Commun.* **1978**, *27*, 325. Kumai, R.; Asamitsu, A.; Tokura, T. *J. Am. Chem. Soc.* **1998**, *120*, 8263. Marks, T. J. *J. Am. Chem. Soc.* **1989**, *111*, 5259.

Table 3. Crystal Data and Experimental Details for α-$ET_3(CoCl_4)_{1-x}(GaCl_4)_x$(TCE) [$x$ = 0.0, 0.62, 0.57, 0.54]

	α-$ET_3(CoCl_4)$(TCE)	α-$ET_3(CoCl_4)_{0.38}(GaCl_4)_{0.62}$(TCE)	α-$ET_3(CoCl_4)_{0.43}(GaCl_4)_{0.57}$(TCE)	α-$ET_3(CoCl_4)_{0.46}(GaCl_4)_{0.54}$(TCE)
empirical formula	$C_{32}H_{27}CoCl_7S_{24}$	$C_{32}H_{27}Co_{0.38}Ga_{0.62}Cl_7S_{24}$	$C_{32}H_{27}Co_{0.43}Ga_{0.57}Cl_7S_{24}$	$C_{32}H_{27}Co_{0.46}Ga_{0.54}Cl_7S_{24}$
fw	1488.11	1494.80	1494.26	1493.93
shape	black plate	black plate	black plate	black plate
crystal system	monoclinic	orthorhombic	orthorhombic	orthorhombic
space group	$P2_1/n$ (no. 14)	$P2_12_12_1$ (no. 19)	$P2_12_12_1$ (no. 19)	$P2_12_12_1$ (no. 19)
a/Å	12.69(3)	13.22(1)	13.27(2)	13.31(3)
b/Å	11.832(6)	36.951(9)	36.90(1)	36.88(2)
c/Å	35.32(1)	11.146(5)	11.095(9)	11.089(7)
α/deg	90	90	90	90
β/deg	94.98(7)	90	90	90
γ/deg	90	90	90	90
V/Å^3	5285(12)	5444(6)	5433(9)	5444(11)
Z	4	4	4	4
R/R_w	0.091/0.083	0.064/0.045	0.070/0.059	0.093/0.079
D_c/g cm^{-3}	1.87	1.82	1.83	1.82
temp/K	298	298	298	298
no. of reflns used	4674/15885	2125/8500	3537/8716	3462/11461
	$\|I_0\| > 3\sigma\|I_0\|$	$\|I_0\| > 3\sigma\|I_0\|$	$\|I_0\| > 3\sigma\|I_0\|$	$\|I_0\| > 3\sigma\|I_0\|$
$2\theta_{max}$/deg	60	60	60	60
λ/Å	0.71073	0.71073	0.71073	0.71073
reference	this work	this work	this work	this work

Table 4. Crystal Data and Experimental Details for β'-$ET_3(CoCl_4)_{2-x}(GaCl_4)_x$ (x = 0.88, 0.66) and β'-$ET_3(MCl_4)_2$ (M = Mn, Zn)

	β'-$ET_3(CoCl_4)_{1.12}(GaCl_4)_{0.88}$	β'-$ET_3(CoCl_4)_{1.34}(GaCl_4)_{0.66}$	β'-$ET_3(MnCl_4)_2$	β'-$ET_3(ZnCl_4)_2$
empirical formula	$C_{30}H_{24}Co_{1.12}\ Ga_{0.88}Cl_4S_{24}$	$C_{30}H_{24}Co_{1.34}\ Ga_{0.66}Cl_4S_{24}$	$C_{30}H_{24}Mn_2Cl_8S_{24}$	$C_{30}H_{24}Zn_2Cl_8S_{24}$
fw	1423.13	1420.76	1547.46	1568.51
shape	black long plate	black long plate		black long plate
crystal system	triclinic	triclinic	triclinic	triclinic
space group	$P\bar{1}$ (no. 2)	$P\bar{1}$ (no. 2)	$P\bar{1}$ (no. 2)	$P\bar{1}$ (no. 2)
a/Å	9.673(5)	9.641(4)	9.714(1)	9.641(1)
b/Å	21.14(1)	20.925(7)	20.595(2)	20.404(3)
c/Å	6.730(7)	6.748(4)	6.802(1)	6.817(1)
α/deg	91.30(7)	90.82(4)	89.70(1)	90.07(1)
β/deg	102.34(6)	101.99(4)	101.66(1)	101.5(1)
γ/deg	85.64(4)	85.91(4)	93.75(1)	86.44(1)
V/Å^3	1340(2)	1328(1)	1329.8(3)	1311.3(4)
Z	1	1	1	1
R/R_w	0.114/0.077	0.085/0.068	0.033	0.041/0.035
D_c/g cm^{-3}	1.94	1.95	1.93	1.99
temp/K	298	298		298
no. of reflns used	1340/6395	1279/6336	3479	4562/7657
	$\|I_0\| > 3\sigma\|I_0\|$	$\|I_0\| > 3\sigma\|I_0\|$	$\|I_0\| > 3\sigma\|I_0\|$	$\|I_0\| > 3\sigma\|I_0\|$
$2\theta_{max}$/deg	60	60		60
λ/Å	0.71073	0.71073		0.71073
reference	this work	this work	25	This work, 26

substitution of $(GaCl_4)^-$ by $(CoCl_4)^{2-}$ in an anion blocking sheet. The anions, $(GaCl_4)^-$ and $(CoCl_4)^{2-}$, are of similar tetrahedral shape and have different charges. Actually, the band-filling control has been carried out for various kinds of electronic ground states. The obtained doped crystals are classified as follows: (1) 2:1 salts, λ-$ET_2(GaCl_4)_{1-x}(CoCl_4)_x$, doping to the antiferromagnet, (2) 2:1 salts, δ'-$ET_2(GaCl_4)_{1-x}(CoCl_4)_x$, doping to the spin gap material, (3) 3:1 salts, α-$ET_3(CoCl_4)_{1-x}(GaCl_4)_x$-(TCE), doping to the charge-ordering system, and (4) 3:2 salts, β'-$ET_3(CoCl_4)_{2-x}(GaCl_4)_x$, doping to the gapless band insulator.

So far, the electronic states of organic conductors including the superconducting state can be regulated only by electron correlation control (U/W), which is the vertical vector as shown in Figure 1.[18] By our successful band-filling control (δ), the electronic state has been reached not only by vertical but also by horizontal control. In this paper, the first systematic study of band-filling control in organic conductors is reported by describing their preparations as single crystals, crystal and band structures, and electrical conducting behaviors at ambient and in pressurized conditions.

Experimental Section

Synthesis. Single crystals were prepared by the electrocrystallization of ET (30 mg) in the presence of TBA·$GaCl_4$ and TBA_2CoCl_4 in 1,1,2-trichloroethane (100 mL) under an inert atmosphere (N_2).[19] The constant current of 0.5 μA was kept at 20 °C. The obtained crystals were washed with MeOH and air-dried at room temperature. The doping content (x) of the obtained crystals depends on the crystal phases. Every x value is totally different from the nominal ratio of electrolytes as shown in Table 1. However, with an increase of the nominal ratio, the doping content also increases systematically. In the same batch, various kinds of crystal phases have been grown. To check the crystal phase and its property, the electrical resistivity was measured after a single crystal was taken from a batch, the lattice parameter of the crystal was checked by the X-ray analysis, and then the doping content of the crystal for 3000 s was determined by EDX measurement. The doping of $(ZnCl_4)^{2-}$ as well as $(CoCl_4)^{2-}$ was similarly carried out (Table 1).

(18) Imada M.; Fujimori, A.; Tokura, Y. *Rev. Mod. Phys.* **1998**, *70*, 1059.

(19) Mori, H. *Int. J. Mod. Phys. B* **1994**, *8*, 1.

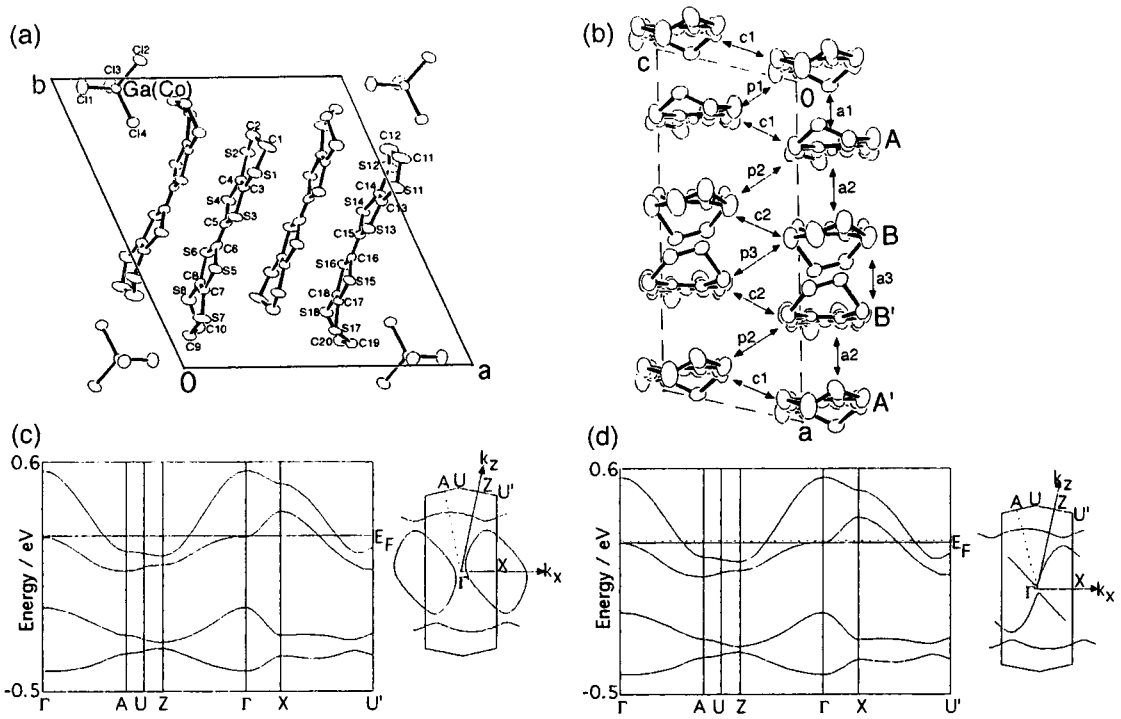

Figure 2. (a) Crystal structure, (b) donor arrangement, and calculated band structures for (c) λ-ET_2GaCl_4 and (d) λ-$ET_2(GaCl_4)_{1-x}(CoCl_4)_x$ (solid line, $x = 0.05$; dotted line, $x = 0.0$).

Crystal and Band Structure Determination. The X-ray diffraction data were collected on a Rigaku AFC5R diffractometer (λ(Mo Kα) = 0.71073 Å, 50 kV, 150 mA, $2\theta \leq 60°$, $\omega-2\theta$ scan technique) and corrected for the usual Lorentz and polarization effects. The data collection conditions and crystal data are listed in Tables 2−4. The crystal structures were solved by a direct method (SHELXS86[21]). The non-hydrogen atoms were refined anisotropically by a least-squares procedure. Hydrogen atoms were included but not refined. The occupancy probabilities of Ga, Co, and Zn atoms were investigated by inductively couple plasma (ICP) (ICP atomic emission spectrometer, SRS1700HVR, SEIKO Instruments Inc.) and energy-dispersive X-ray (EDX) (EDX microanalyzer, JED-2001, JEOL Datum Ltd.) measurements. Both values are consistent with each other.

The overlap integrals were calculated by the extended Hückel method (Tables 5, 7, and 9), and the tight binding band calculations were carried out on the basis of the transfer integrals (t) proportional to overlap integrals (S): $t = ES$, where E is constant of −10.0 eV. [22]

Physical Properties. The electrical resistivity was measured by the conventional four-probe method with application of a low dc current of 10−1000 μA in the range from 300 to 1.3 K. Gold wires (Tanaka Kikinzoku, 16 or 18 $\mu\phi$) were attached to a crystal with gold paste (Tokuriki Chemicals, no. 8560) as electrodes. Pressure dependence was measured by using a clamp-type cell with an oil (Daphne no. 7373) as a pressure medium. The pressure was determined from the resistance of a manganin wire.

Results and Discussion

2:1 Salts [λ-$ET_2(GaCl_4)_{1-x}(MCl_4)_x$ and δ'-$ET_2(GaCl_4)_{1-x}(MCl_4)_x$ [M = Co, Zn]]. The crystal structure of λ-ET_2GaCl_4 is shown in Figure 2. The unit cell contains four donors and two anions, and they are located on the general positions. The crystallographically independent molecules are two ET molecules and one $(GaCl_4)^-$. The two-dimensional layered structure is composed of alternate stacking of the donor layer and the anion sheet along the b-axis. In the insulating anion layer, λ-$ET_2(GaCl_4)_{0.95}(CoCl)_{0.05}$, a tetrahedral MCl_4 anion, allocated in the general position, is composed of 5% $(CoCl_4)^{2-}$ and 95% $(GaCl_4)^-$. In the donor layer, two dimers (AB, B′A′; a2) form 4-fold ET donors along the a-axis as shown in Figure 2b and Table 5. The strong donor dimerization splits the energy band to the upper and lower ones as shown in Figure 2c. When we assume only the upper energy bands ($x = 0.0$), the effective half-filled band is realized. The slight band-filling control ($x = 0.05$) changes the Fermi surface from the closed orbit around X (Figure 2c) to the open one-dimensional nature along the c-direction (Figure 2d). Since the electronic ground state of λ-ET_2GaCl_4 is an antiferromagnetic state,[6] the prepared λ-$ET_2(GaCl_4)_{1-x}(CoCl_4)_x$ is a band-filling control for the antiferromagnetic Mott insulator.

On the other hand, though δ'-ET_2GaCl_4 has the same 2:1 stoichiometry, the electronic ground state is a nonmagnetic insulator.[23] The crystal structure of δ'-$ET_2(GaCl_4)_{0.95}(CoCl_4)_{0.05}$ is shown in Figure 3. This salt also has four donors and two

Table 5. Overlap Integrals ($\times 10^{-3}$) for λ-ET_2GaCl_4 and δ'-ET_2GaCl_4

overlap integral	λ-ET_2GaCl_4	overlap integral	δ'-ET_2GaCl_4
a1	9.3	a1	−3.9
a2	−25.8	a2	24.2
a3	8.1	a3	23.4
c1	−4.6	c1	−0.9
c2	−2.8	c2	6.9
p1	12.0	p	4.8
p2	−6.1	q	4.3
p3	1.8	r	−2.4

(20) Montgomery, L. K. Personal communication.
(21) Sheldrick, G. H. *Crystallographic Computing 3*; Oxford University Press: Oxford, 1985; pp 175−189.
(22) Mori, T.; Kobayashi, A.; Sasaki, Y., Kobayashi, H.; Saito, G.; Inokouchi, H. *Bull. Chem. Soc. Jpn.* **1984**, *57*, 627. The parameters of Slater atomic orbitals [z exponent, ionization potential (eV)] are as follows: S, 3s (2.112, −20.0), 3p (1.825, −11.0), 3d (1.5, −5.44); C, 2s (1.625, −21.4), 2p (1.625, −11.4); H, 1s (1.0, −13.6).

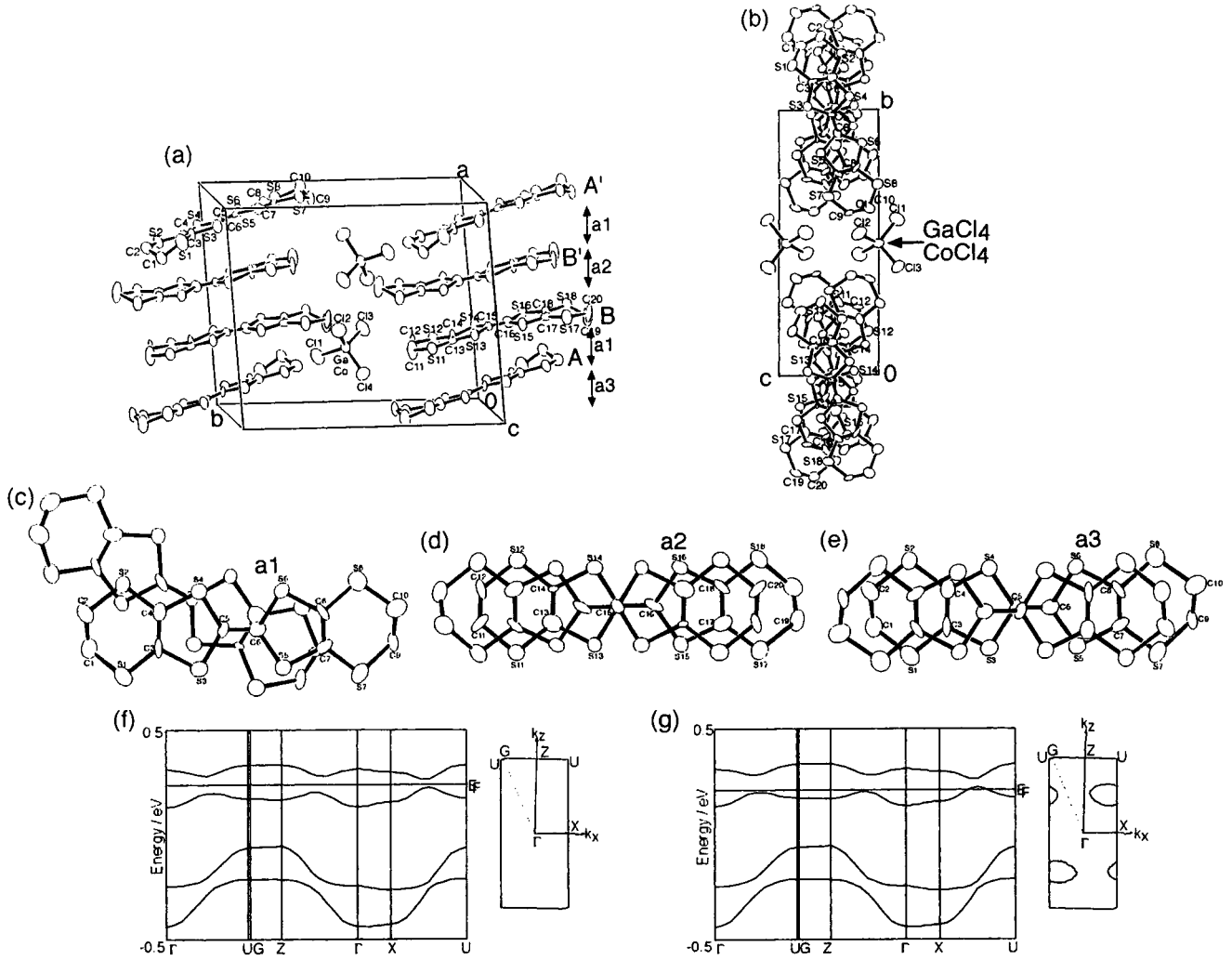

Figure 3. (a) Crystal structure, (b) donor arrangement, overlaps of molecules [(c) a1, (d) a2, (e) a3] ($x = 0.05$), and calculated band structure [(f) $x = 0.0$, (g) $x = 0.14$] for δ'-$ET_2(GaCl_4)_{1-x}(CoCl_4)_x$.

anions in a unit cell, and ET molecules and ions are located on the general positions. The crystallographically independent molecules are two ET molecules and one $[(GaCl_4)^-_{0.95}(CoCl_4)^{2-}_{0.05}]$. The donor layer and anion sheet stack along the *b*-axis. In the anion layer, 5% $(CoCl_4)^{2-}$ and 95% $(GaCl_4)^-$ form tetrahedral MCl_4. In the donor sheet, the dimerized ET [AA′ (a3; Figure 3a,e), BB′ (a2; Figure 3a,d)] stack in a twisted manner by $\omega \approx 26°$ (a1; Figure 3a,c) along the *a*-axis. The calculated energy bands of δ'-$ET_2(GaCl_4)_{1-x}(CoCl_4)_x$ [$x = 0.0$, 0.14] are depicted in Figure 3f,g, respectively. Whereas δ'-ET_2GaCl_4 is a band insulator so that no Fermi surface is obtained, δ'-$ET_2(GaCl_4)_{0.86}(CoCl_4)_{0.14}$ indicates a semimetallic band structure, where small hole and electron pockets appear.

The temperature dependences of electrical resistivity for δ'-$ET_2(GaCl_4)_{1-x}(MCl_4)_x$ [$x = 0.0$, 0.05 (M = Co), 0.14 (M = Zn)] and λ-$ET_2(GaCl_4)_{1-x}(MCl_4)_x$ [$x = 0.0$, 0.05 (M = Co), 0.06 (M = Zn)] are depicted in Figure 4. Upon doping to δ'-ET_2GaCl_4 by 14%, the resistivity at room temperature decreases from 10 to 0.3 Ω cm, and the doped sample shows semiconducting behavior. As for λ-type salts, the 6 % doped sample reduces the room temperature resistivity from 3 to 0.1 Ω cm and a similar semiconducting behavior was observed. The

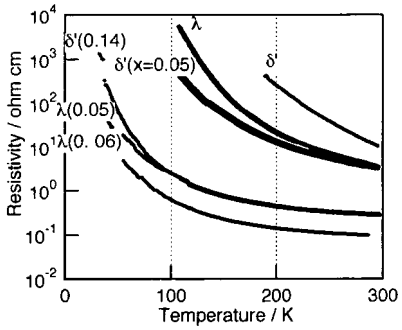

Figure 4. Electrical resistivities of δ'-$ET_2(GaCl_4)_{1-x}(MCl_4)_x$ [$x = 0.0$, 0.05 (M = Co), 0.14 (M = Zn)] and λ-$ET_2(GaCl_4)_{1-x}(MCl_4)_x$ [$x = 0.0$, 0.05 (M = Co), 0.06 (M = Zn)].

resistivity decreases gradually by an increase of the doping degree for both salts, and the doping effect of the λ-phase is stronger than that of the δ'-phase.

3:1 Salts [α-$ET_3(CoCl_4)_{1-x}(GaCl_4)_x$(TCE)]. The crystal structure of α-ET_3CoCl_4(TCE) is shown in Figure 5. The unit cell contains twelve ET molecules, four $(CoCl_4)^{2-}$ anions, and four TCE solvents. Three crystallographically independent ET molecules (A, B, C), $(CoCl_4)^{2-}$, and TCE are on general positions. The anion layer consists of $(CoCl_4)^{2-}$ and TCE, and the donor sheet stacks along the *c*-axis (Figure 5a). The projected

(23) Yoneyama, N.; Miyazaki, A.; Enoki, T.; Saito, G. *Bull. Chem. Soc. Jpn.* **1999**, *72*, 639.

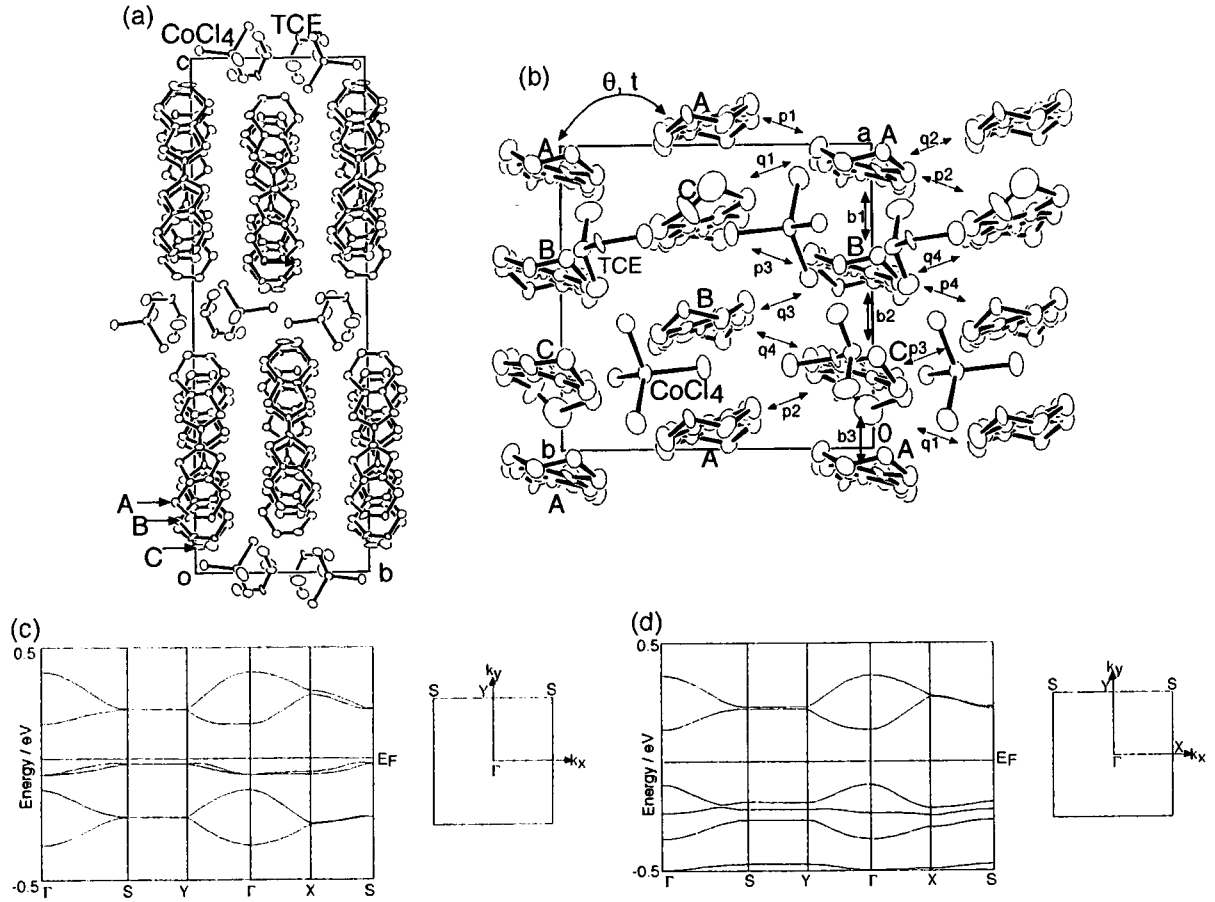

Figure 5. (a) Crystal structure, (b) donor and anion arrangement, and calculated band structures (c) without consideration of charge ordering and (d) with consideration of charge ordering for α-ET_3CoCl_4(TCE).

Table 6. Central C═C Bond Lengths (Å) of ET for α-$ET_3(CoCl_4)_{1-x}(GaCl_4)_x$(TCE) [$x$ = 0.0, 0.62, 0.57, 0.46; ET_3 = ABC] at 298 K

α-$ET_3(CoCl_4)$(TCE)		α-$ET_3(CoCl_4)_{0.38}(GaCl_4)_{0.62}$(TCE)		α-$ET_3(CoCl_4)_{0.43}(GaCl_4)_{0.57}$(TCE)		α-$ET_3(GaCl_4)_{0.54}(CoCl_4)_{0.46}$(TCE)	
charge of ET	C═C bond length	charge of ET	C═C bond length	charge of ET	C═C bond length	charge of ET	C═C bond length
C	1.301	C	1.305				
0	1.31	0	1.31	0	1.31	0	1.31
A	1.356	A	1.329	B	1.349	A	1.358
		B	1.358	C	1.351		
				A	1.359		
0.5	1.365	0.5	1.365	0.5	1.365	0.5	1.365
2/3	1.366	2/3	1.366	2/3	1.366	2/3	1.366
B	1.374					C	1.370
						B	1.376
1	1.38	1	1.38	1	1.38	1	1.38

[a] Reference 28. [b] Reference 29. [c] Reference 30. [d] Reference 31. [e] Reference 32.

view of both layers is shown in Figure 5b. In the anion layer, $(CoCl_4)^{2-}$ and TCE are arranged alternately in the two-dimensional plane. As for the donor sheet, the central C═C bond lengths of donors A, B, and C suggest that the charge ordering occurs at room temperature: $A^{\delta+}$, B^+, and C^0 (Table 6). The neutral donor, C^0, is surrounded by $A^{\delta+}$ and B^+. The distances less than the van der Waals radii between ET molecules and anions [r(Cl−H) = 2.87 Å, r(Cl−C) = 3.37 Å, r(Cl−S) = 3.47 Å] are found: four contacts between the $A^{\delta+}$ molecule and anion, four around B^+, and one around C^0. The close contacts appear around $A^{\delta+}$ and B^+, which have positive charges, in which the Coulomb interactions between donor cations and anions are one of the important factors in determining the pattern of charge ordering.

The donor arrangement of α-ET_3CoCl_4(TCE) is α-type, where the dihedral angles between donor molecules (θ) are 146−148 °. The band calculation based upon the crystal structure analysis is shown in Figure 5c,d without ($A^{2/3+}$, $B^{2/3+}$, $C^{2/3+}$) and with (A^+, B^+, C^0) consideration of charge ordering, respectively. Both energy bands indicate band insulators. The resistivity of α-ET_3CoCl_4(TCE), however, shows metallic behavior down to 165 K (Figure 8, x = 0.0). The disagreement of the band-insulating nature and the semimetallic behavior may come from the overestimation of the band calculation due to the difficult estimation of the α-phase.

The 3-fold donor stacking structure in a charge-ordering state of α-ET_3CoCl_4(TCE) is similar to that of α-ET_3CuBr_4.[24] The anion charge of α-ET_3CuBr_4 is also $(CuBr_4)^{2-}$. The resistivity

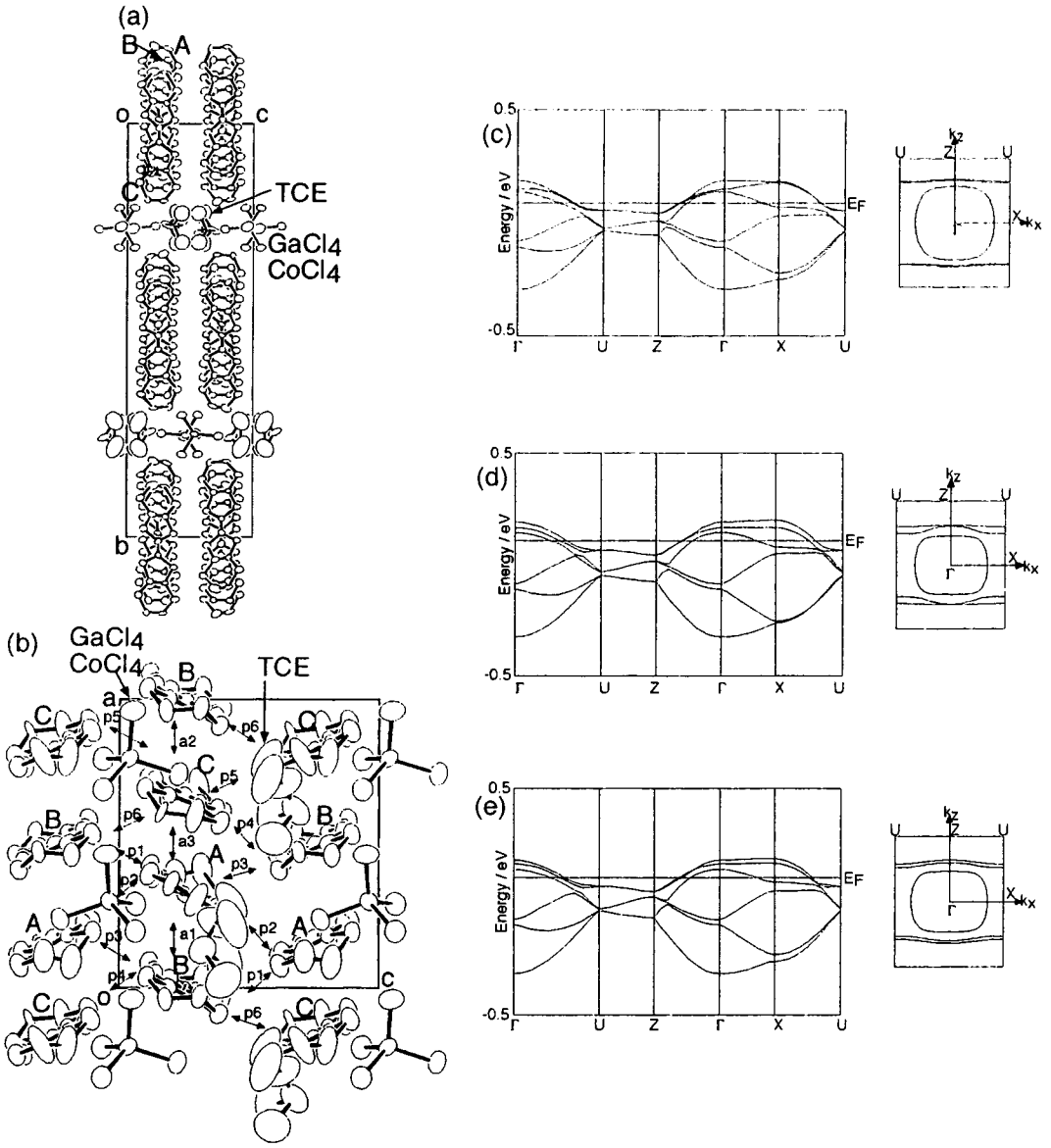

Figure 6. (a) Crystal structure, (b) donor and anion arrangement ($x = 0.57$), and calculated band structures [(c) $x = 0.62$, (d) $x = 0.57$, (e) $x = 0.54$] for α-$ET_3(CoCl_4)_{1-x}(GaCl_4)_x$(TCE).

at room temperature is relatively low, 0.6 Ω cm, even though ET donors are in a charge-ordering state such as α-(ET^+ET^+-ET^0)$CuBr_4$. The semiconducting behavior is observed with 0.17 eV, which is in contrast to the metallic behavior of α-ET_3CoCl_4-(TCE) down to 165 K.

By doping $(GaCl_4)^-$ to α-ET_3CoCl_4(TCE), the obtained α-$ET_3(CoCl_4)_{1-x}(GaCl_4)_x$(TCE) also has an α-type donor arrangement, but the space group is $P2_12_12_1$, which is different from that of α-ET_3CoCl_4(TCE), $P2_1/n$, owing to the different anion arrangement. As shown in Figure 6a, the donor sheet and anion layer stack along the *b*-axis, and the projected figure to the *ac* plane is depicted in Figure 6b. The anions [$(CoCl_4)^{2-}{}_{1-x}$-$(GaCl_4)^-{}_x$] and solvent TCE are aligned along the *a*-axis. This is in contrast to the anions and the solvent of α-$ET_3(CoCl_4)$-(TCE) being arranged alternately in the two-dimensional *ab* plane. In the donor sheet, the crystallographically independent donors are A, B, and C. The charges of A, B, and C, indicated by the central C═C bond length of the donors, are shown in Table 6, and the *x* dependence of the ET charges for α-ET_3-$(CoCl_4)_{1-x}(GaCl_4)_x$(TCE) is summarized in Figure 7. The *x* values are determined by ICP and EDX measurements. The ICP measurement indicates $x = 0.54(1)$, $0.57(1)$, and $0.62(1)$, which are consistent with $x = 0.55$, $0.57(0)$, and $0.63(1)$ for 3000 s counts by the EDX measurements. With increasing *x* of

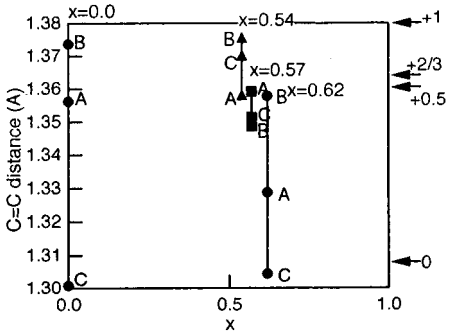

Figure 7. Doping (*x*) dependence of ET charge for α-$ET_3(CoCl_4)_{1-x}$-$(GaCl_4)_x$(TCE) [$x = 0.0$, 0.62, 0.57, 0.54].

(24) Mori, T.; Sakai, F.; Saito, G.; Inokuchi, H. *Chem. Lett.* **1987**, 927.

Table 7. Overlap Integrals ($\times 10^{-3}$) for α-$ET_3(GaCl_4)_{1-x}(CoCl_4)_x$(TCE) [$x = 0.0, 0.62, 0.57, 0.46$]

overlap integral	α-$ET_3(CoCl_4)$(TCE)	overlap integral	α-$ET_3(CoCl_4)_{0.38}(GaCl_4)_{0.62}$(TCE)	α-$ET_3(CoCl_4)_{0.43}(GaCl_4)_{0.57}$(TCE)	α-$ET_3(GaCl_4)_{0.54}(CoCl_4)_{0.46}$(TCE)
b1	−22.4	a1	2.8	2.7	3.5
b2	−3.2	a2	2.1	3.8	−3.3
b3	−0.1	a3	2.9	3.8	−3.4
p1	5.8	p1	6.6	7.1	6.6
p2	8.3	p2	6.5	6.8	6.8
p3	2.7	p3	5.5	5.9	5.9
p4	5.8	p4	7.4	6.8	−7.1
q1	3.4	p5	4.7	5.0	4.6
q2	5.8	p6	5.6	6.5	−6.0
q3	5.8				
q4	3.0				

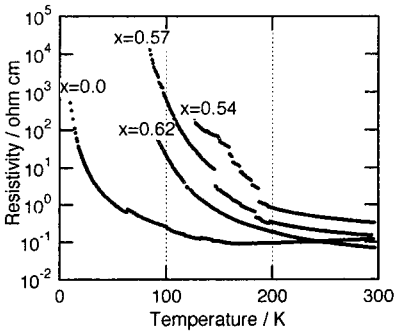

Figure 8. Electrical resistivities of α-$ET_3(CoCl_4)_{1-x}(GaCl_4)_x$(TCE) [$x = 0.0, 0.54, 0.57, 0.62$].

$(GaCl_4)^-$ from 0.54, to 0.57, and to 0.62, the average charge of the ET donors decreases (Figure 7). Since each donor, A, B, and C, is aligned along the *c*-axis, the same charges are arranged horizontally, namely, static stripe-type charge ordering (Figure 6b). On the other hand, the charge ordering of α-ET_3CoCl_4-(TCE) spreads in the two-dimensional plane due to different anion arrangements.

The overlap integrals and band structures based upon band structures are shown in Table 7 and Figure 6c−e. The overlap integrals along the donor stacking direction (a1, a2, and a3) are almost the same value. Accordingly, the donor arrangement is very similar to *θ*-type, a so-called 3-fold *θ*-type salt. The crystal structure reflects the band structure. The Fermi surface of *θ*-type salts has a closed orbit. The 3-fold Fermi surfaces along the *a*-axis, which originates from the *θ*-type closed orbit, were obtained for α-$ET_3(CoCl_4)_{1-x}(GaCl_4)_x$(TCE) [$x = 0.62$, 0.57, 0.54], which are structures similar to one another. The dihedral angles of the donors are 126−131° ($x = 0.62$), 126−129° ($x = 0.57$), and 126−129° ($x = 0.54$), respectively. The large dihedral angles and the calculated narrow bandwidth, 0.52−0.56 eV, are consistent with semiconducting behaviors. The temperature dependences of the resistivities are shown in Figure 8. The room-temperature resistivities are 0.07−0.3 Ω cm, and with an increase of *x* from 0.54, to 0.57, and to 0.62, the resistivity decreases gradually.

3:2 Salts [*β′*-$ET_3(CoCl_4)_{2-x}(GaCl_4)_x$]. As shown in Table 4, *β′*-$ET_3(CoCl_4)_{2-x}(GaCl_4)_x$ [$x = 0.66$, 0.88] is isostructural to *β′*-$ET_3(MCl_4)_2$ (M = Mn,[25] Zn[26]). A unit cell contains three ET donors and two anions. Since one ET molecule (A) and one anion are on general positions, and the other ET molecule (B) is on an inversion center, the crystallographically independent molecules are 1.5 ET molecules and one anion. The donor layer and the hybrid sheet, composed of anions and donors, stack along the *b*-axis (Figure 9a). In the donor layer, the donor arrangement is *β′*; the dimerized donors (A and A′; a1) stack along the 30° (a2) and the 60° (q) directions (Figure 9b). In the hybrid sheet, donors make a one-dimensional chain (c2), whereas anions [$(CoCl_4)^{2-}$, $(GaCl_4)^-$] sandwich the donor array (Figure 9a,c). The interactions between donors in the donor layer (A) and hybrid sheet (B), s1 (0.1×10^{-3}) and s2 (-0.2×10^{-3}), are very small.

To estimate the charge of ET, the central C═C bond lengths are listed in Table 8. The parent material is in a charge-ordering state such as *β′*-$(A^+A^+B^{2+})(MnCl_4)_2$; the B^{2+} is in a hybrid sheet, composed of anions and donors, whereas A^+ donors form a two-dimensional donor layer. The estimated charge is in good agreement with those obtained by P. Guionneau's method[27] ($A^{0.90+}$ and $B^{1.87+}$) within the error due to the high oxidation state. Upon doping to the parent material by a partial substitution of a 2− anion, $(CoCl_4)^{2-}$, by a 1− anion, $(GaCl_4)^-$, *β′*-$ET_3(CoCl_4)^{2-}{}_{2-x}(GaCl_4)^-{}_x$ [$x = 0.66$, 0.88] has been obtained. As for $x = 0.66$, the charge of B is close to 2+, and that of A is between 0 and 1+ on the basis of the bond length (Table 8). We checked that there was no 3-fold periodicity by the X-ray photograph measurement at room temperature. The calculated overlap integrals of *β′*-$ET_3(CoCl_4)_{2-x}(GaCl_4)_x$ are summarized in Table 9. By use of these overlap integrals, the band dispersion and Fermi surface of the donor layer (A) and the donor array in the hybrid sheet (B) of the parent material, *β′*-$(A^+A^+B^{2+})(MnCl_4)_2{}^{2-}$, are calculated as shown in Figure 9d,e. Since the A^+ donors are dimerized and the overlap integrals between dimers are large enough, the dispersion of the gapless band insulator is relatively large, but no Fermi surface is obtained. The total bandwidth is around 1.1 eV owing to the gapless band feature. When the charge of B remains as 2+ and the A site is electron-doped on the basis of the bond length of ET, the calculated Fermi surface of *β′*-$(A^{0.67+}A^{0.67+}B^{2+})(CoCl_4)^{2-}{}_{1.34}(GaCl_4)^-{}_{0.66}$ is depicted in Figure 9f,g. The one-dimensional band structure at the A site is obtained. If both A and B sites are assumed to be electron-doped as *β′*-$(A^{0.92+}A^{0.92+}B^{1.5+})$-

(25) Mori, T.; Inokuchi, H. *Bull. Chem. Soc. Jpn.* **1988**, *61*, 591.
(26) Shibaeva, R. P.; Lobkovskaya, R. M.; Korotkov, V. E.; Kuahxh, N. D.; Yagubskii, E. B.; Makova, M. K. *Synth. Met.* **1988**, *27*, A457.
(27) Guionneau, P.; Kepert, C. J.; Bravic, G.; Chasseau, D.; Truter, M. R.; Kurmoo, M.; Day, P. *Synth. Met.* **1997**, *85*, 1973.
(28) Kobayashi, H.; Kobayashi, A.; Sasaki, Y.; Saito, G.; Inokuchi, H. *Bull. Chem. Soc. Jpn.* **1986**, *59*, 301.
(29) Kobayashi H.; Kato, R.; Mori, T.; Kobayashi, A.; Sasaki, Y.; Saito, G.; Inokuchi, H. *Chem. Lett.* **1983**, 759.
(30) Kobayashi, H.; Kato, R.; Mori, T.; Kobayashi, A.; Sasaki, Y.; Saito G.; Enoki, T.; Inokuchi, H. *Chem. Lett.* **1984**, 179.
(31) Kobayashi, H.; Kobayashi, A.; Sasaki, Y.; Saito, G.; Inokuchi, H. *Chem. Lett.* **1984**, 183.
(32) Abboud, K. A.; Clevenger, M. B.; de Oliveira, G. F.; Talham, D. R. *J. Chem. Soc., Chem. Commun.* **1993**, 1560.

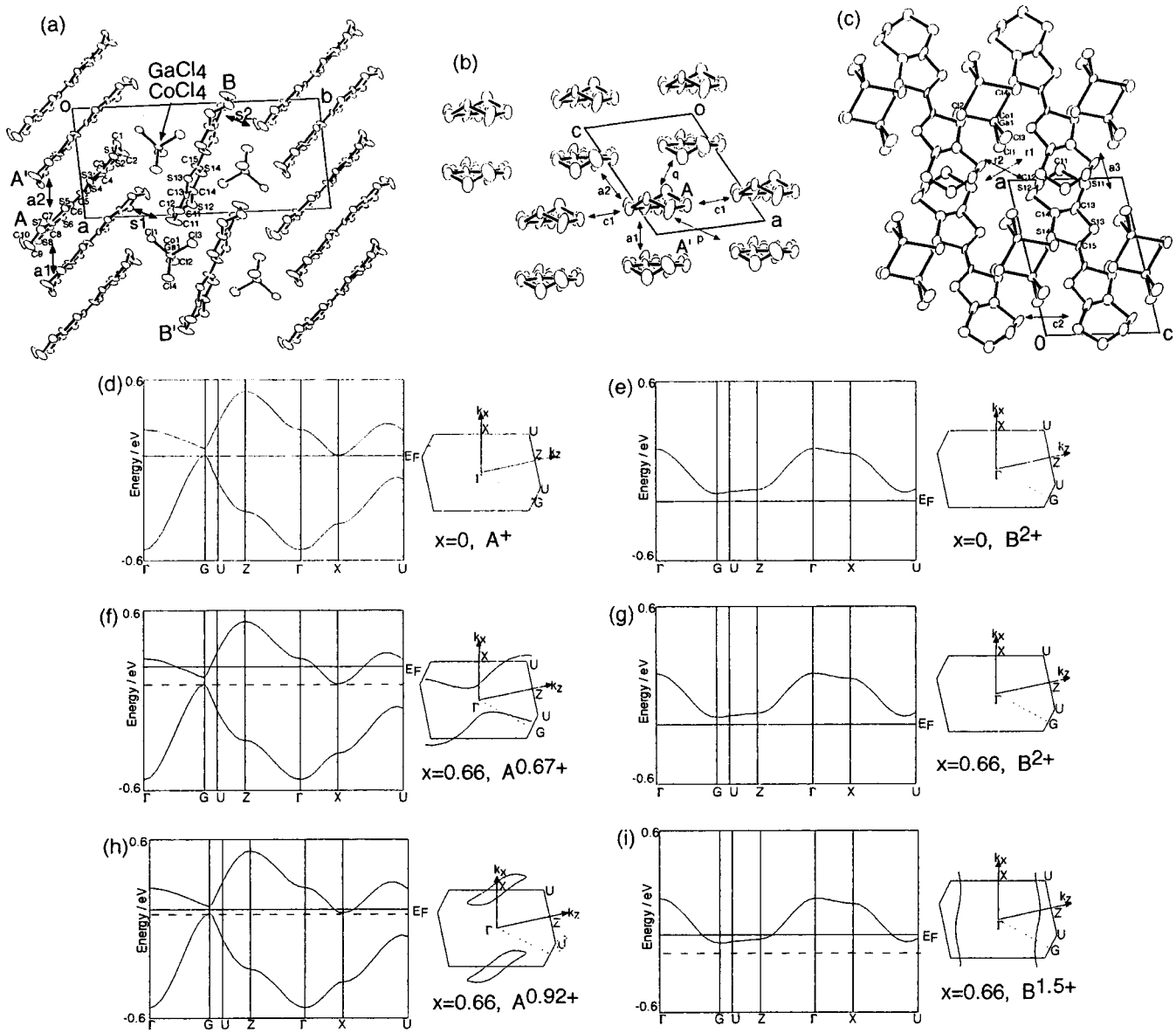

Figure 9. (a) Crystal structure, (b) donor arrangement, (c) donor and anion arrangement, and calculated band structure for β'-$(ET^{+}ET^{+}ET^{2+})(MnCl_4)_2$ [(d) ET^{+}, (e) ET^{2+}], β'-$(ET^{0.67+}ET^{0.67+}ET^{2+})(CoCl_4)_{1.34}(GaCl_4)_{0.66}$ [(f) $ET^{0.67+}$, (g) ET^{2+}], and β'-$(ET^{0.92+}ET^{0.92+}ET^{1.5+})(CoCl_4)_{1.34}(GaCl_4)_{0.66}$ [(h) $ET^{0.92+}$, (i) $ET^{1.5+}$].

Table 8. Central C=C Bond Lengths (Å) of ET for β'-$ET_3(CoCl_4)_{1.34}(GaCl_4)_{0.66}$ and β'-$ET_3(MnCl_4)_2$ [ET_3 = AAB] at 298 K

β'-$ET_3(CoCl_4)_{1.34}(GaCl_4)_{0.66}$		β'-$ET_3(MnCl_4)_2$	
charge of ET	C=C bond length	charge of ET	C=C bond length
0	1.31[a]	0	1.31[a]
A	1.332		
0.5	1.365[b]	0.5	1.365[b]
2/3	1.366[c]	2/3	1.366[c]
1	1.38[d]	1	1.38[d]
		A	1.381(6)
		B	1.431(7)
2	1.439[e]	2	1.439[e]
B	1.488		

[a] Reference 28. [b] Reference 29. *c*Reference 30. [d] Reference 31. [e] Reference 32.

Table 9. Overlap Integrals ($\times 10^{-3}$) of β'-$ET_3(CoCl_4)_{2-x}(GaCl_4)_x$ (x = 0.88, 0.66)

overlap integral	β'-$ET_3(CoCl_4)_{1.12}(GaCl_4)_{0.88}$	β'-$ET_3(CoCl_4)_{1.34}(GaCl_4)_{0.66}$	β'-$ET_3(MnCl_4)_2$
a1	34.2	26.2	27.1
a2	14.4	13.7	14.0
a3	−1.3	−0.8	−1.0
c1	8.3	6.4	6.1
c2	−7.5	−6.7	−5.7
p	6.2	5.3	4.9
q	−3.8	−5.1	−4.3
r1	0.0	0.0	0.0
r2	−0.1	−0.1	−0.2
s1	0.3	0.1	
s2	−0.3	−0.2	
ref	this work	this work	25

$(CoCl_4)^{2-}{}_{1.34}(GaCl_4)^{-}{}_{0.66}$, the obtained band structures are shown in Figure 9h,i, respectively. As a result, the semimetallic and one-dimensional band dispersions were calculated (x = 0.66; $A^{0.92+}$, $B^{1.5+}$). It is curious that the shape of the obtained Fermi surface changes by the band-filling control.

The temperature dependences of the resistivities are shown in Figure 10. Although the calculated band structure of the parent

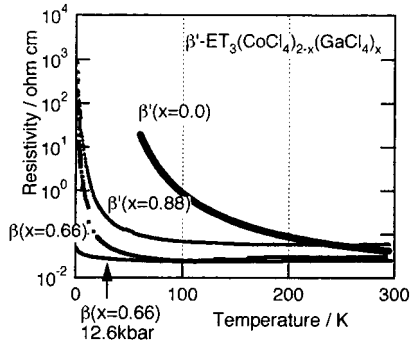

Figure 10. Electrical resistivities for β'-$ET_3(MCl_4)_{2-x}(GaCl_4)_x$ [$x = 0.0$ (M = Mn), 0.88, 0.66 (M = Co)] at an ambient pressure and β'-$ET_3(CoCl_4)_{1.34}(GaCl_4)_{0.66}$ under 12.6 kbar.

material β'-$ET_3(MnCl_4)_2$ is the gapless band insulator, the conductivity at room temperature is relatively high ($\rho_{RT} = 25$ S cm^{-1}, $E_a = 0.04$ eV).[25] The thermally activated electrons or obtained holes could be carriers. By a substitution of $(CoCl_4)^{2-}$ by $(GaCl_4)^-$, the metallic behaviors are observed down to 140 K for $x = 0.88$ and 100 K for $x = 0.66$. The smaller doping material ($x = 0.66$) is more conductive than $x = 0.88$. They are the first metallic behaviors in organic conductors by doping to the gapless band insulator.

To suppress the increase of resistivity at low temperature, not only the band-filling control but also the electron correlation control (U/W) was examined. When the pressure is applied to the conductive one ($x = 0.66$), the increase of resistivity at low temperatures is almost suppressed at 12.6 kbar as shown in Figure 10. A study of the doping dependence in the series of β'-$ET_3(MCl_4)_{1-x}(GaCl_4)_x$ [M = Co, Zn] is in progress.

Band-Filling Effect in Organic Conductors. Finally, let us consider the effect of band-filling control in organic conductors. As for the δ'-phase (2:1 salt), the 4-fold stacking mode, consisting of two dimers, is very similar to that of the λ-phase (2:1 salt) (Figures 2 and 3). Accordingly, two upper bands and two lower bands split each other with a gap of 0.17 eV for both δ'- and λ-ET_2GaCl_4 (Figures 3f and 2c). Since the band dispersion of δ'-ET_2GaCl_4 is very weak, the band-insulating feature is calculated as shown in Figure 3f. The resistivity at room temperature is 10 Ω cm with an activation energy of 0.17 eV. With doping of $(MCl_4)^{2-}$ [$x = 0.14$], the band filling has changed as shown in Figure 3g, and the hole and electron pockets have appeared. The resistivity at room temperature reduces from 10 Ω cm ($x = 0.0$) to 0.3 Ω cm ($x = 0.14$), but the temperature dependence of the resistivity has not changed even after doping.

On the other hand, there has been a relatively large dispersion in λ-ET_2GaCl_4, so that the closed and one-dimensional orbits have appeared (Figure 2c). When we consider only the upper two bands, the *effective* half-filled band has been realized. By doping $(MCl_4)^{2-}$ to this material ($x = 0.05$), the band filling decreases slightly (Figure 2d). Accordingly, the Fermi surface has been modified, and two open orbits have appeared. By the effect of doping to the effective half-filled band, the resistivity at room temperature decreases from 3 Ω cm ($x = 0.0$) to 0.1 Ω cm ($x = 0.05$). The temperature dependence of resistivity seems to be similar even after doping. Since the resistivity decreases by 1/30 by 14% doping for δ'-ET_2GaCl_4 and 6% doping for λ-ET_2GaCl_4, the doping effect is larger for λ-ET_2GaCl_4.

As for the β'-phase, the parent material, β'-$ET_3(MnCl_4)^{2-}{}_2$, is also a gapless band insulator, but since the band dispersion is large, the lowest energy level of the upper band and the highest energy level of the lower one are the same. Therefore, the total bandwidth is 1.1 eV as shown in Figure 9d. This β'-phase (3:2 salt) has a rare crystal structure; the 2− negative anions, $(MnCl_4)^{2-}$, have been sandwiched by the 1+ charged donor sheet (A) and the 2+ charged donor array (B) as shown in Figure 9a. This novel structure allows that ET^+ donors with a large positive charge to stack to form a segregated donor layer. By doping $(GaCl_4)^-$ to β'-$ET_3(CoCl_4)^{2-}{}_2$, single crystals of β'-$ET_3(CoCl_4)_{2-x}(GaCl_4)_x$ [$x = 0.66$, 0.88] have been obtained. As described vide supra, the semiconducting behavior of the parent material, β'-$ET_3(MnCl_4)^{2-}{}_2$, has transferred to a metallic feature down to 140 K ($x = 0.88$) and 100 K ($x = 0.66$) for β'-$ET_3(CoCl_4)_{2-x}(GaCl_4)_x$. The doping to the band insulator without an energy gap is most effective in comparison with those of the λ-phase with an effective half-filled band and the δ'-phase with the band insulator ($E_a = 0.17$ eV). The doping effect of β'-$ET_3(CoCl_4)_{2-x}(GaCl_4)_x$ is rather complicated since there are two kinds of doping sites, a donor sheet (A) and a donor array (B). The C=C bond lengths of ET and the estimation by Guionneau's method[27] for β'-$ET_3(CoCl_4)_{1.34}(GaCl_4)_{0.66}$ suggest doping close to β'-$(A^{0.67+}A^{0.67+}B^{2+})_3(CoCl_4)_{1.34}(GaCl_4)_{0.66}$. The calculated band structures are shown in Figure 9f,g. The actual Fermi surface would be able to be observed by the optical measurements. It is curious that the change of band filling affords the various kinds of Fermi surfaces from one-dimensional to two-dimensional.

Conclusion

The first systematic study of band-filling control in organic conductors has been successfully carried out. By a substitution of $(GaCl_4)^-$ by $(CoCl_4)^{2-}$ in an anion layer, the charge of the ET donor, namely, band filling, changes. By doping $(CoCl_4)^{2-}$ to the 2:1 organic antiferromagnet (λ-ET_2GaCl_4) or 2:1 nonmagnetic insulator (δ'-ET_2GaCl_4), the semiconductors transfer to the more conductive semiconductors. As for the 3:1 salt, α-$ET_3(CoCl_4)_{1-x}(GaCl_4)_x$(TCE) ($x = 0.0$, 0.54, 0.57, 0.62), the pattern of charge ordering of the ET donors has changed. Finally, with doping $(GaCl_4)^-$ to the 3:2 gapless band insulator isostructural to β'-$ET_3(MCl_4)^{2-}{}_2$ (M = Mn, Zn), the metallic organic conductor, β'-$ET_3(CoCl_4)_{2-x}(GaCl_4)_x$ ($x = 0.66$, 0.88), by band-filling control has been obtained. When the pressure is applied to β'-$ET_3(CoCl_4)_{1.34}(GaCl_4)_{0.66}$, the increase of resistivity at low temperatures is almost suppressed at 12.6 kbar.

Acknowledgment. This work is supported by the New Energy and Industrial Technology Development Organization (NEDO).

JA010567V